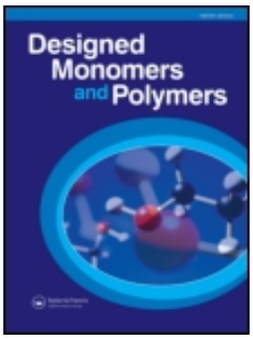

Designed Monomers and Polymers

ISSN: (Print) 1568-5551 (Online) Journal homepage: www.tandfonline.com/journals/tdmp20

Ferrocene clicked polypyrrole derivatives: effect of spacer group on electrochemical properties and post-polymerization functionalization

Pinar Camurlu, Nese Guven & Zeynep Bicil

To cite this article: Pinar Camurlu, Nese Guven & Zeynep Bicil (2016) Ferrocene clicked polypyrrole derivatives: effect of spacer group on electrochemical properties and post-polymerization functionalization, Designed Monomers and Polymers, 19:3, 212-221, DOI: 10.1080/15685551.2015.1136526

To link to this article: https://doi.org/10.1080/15685551.2015.1136526

DESIGNED MONOMERS AND POLYMERS, 2016
VOL. 19, NO. 3, 212–221
http://dx.doi.org/10.1080/15685551.2015.1136526

Taylor & Francis
Taylor & Francis Group

Ferrocene clicked polypyrrole derivatives: effect of spacer group on electrochemical properties and post-polymerization functionalization

Pinar Camurlu, Nese Guven and Zeynep Bicil

Department of Chemistry, Akdeniz University, Antalya, Turkey

ABSTRACT

In this study, novel ferrocene-functionalized N-alkyl substituted pyrrole derivatives, namely 4-ferrocenyl-1-[3-(pyrrol-1-yl)propyl]-1*H*-1,2,3-triazole (Py3Fc), 4-ferrocenyl-1-[4-(pyrrol-1-yl)butyl]-1*H*-1,2,3-triazole (Py4Fc), and 4-ferrocenyl-1-[6-(pyrrol-1-yl)hexyl]-1*H*-1,2,3-triazole (Py6Fc), were synthesized via click reaction and the monomers were characterized by ^{1}H NMR, ^{13}C NMR, FTIR, and HRMS techniques. Redox properties of the monomers were investigated by cyclic voltammetry (CV) studies. Contrary to general literature, both Py4Fc and Py6Fc were electrochemically polymerized without loss in redox activity of ferrocene group. Moreover, click chemistry was utilized in post-polymerization functionalization. For this purpose, three azide-containing polypyrroles, P(Py3N$_3$), P(Py4N$_3$), and P(Py6N$_3$) were electrochemically synthesized and subjected to click reaction in the presence of ethynylferrocene. CV studies of the post-polymerization functionalized polymers revealed quasi-reversible waves, while only P(Py6-post-Fc) showed the characteristic redox behavior of both polypyrrole and ferrocene. Thus, in this study preparation of a conducting homopolymers of pyrrole having covalently bonded ferrocene units was demonstrated and effect of spacer group is investigated.

ARTICLE HISTORY
Received 22 July 2015
Accepted 23 December 2015

KEYWORDS
Click chemistry; ferrocene; pyrrole; electrochemical polymerization; post-polymerization functionalization

1. Introduction

Research interest in polypyrrole derivatives have increased significantly due to versatility of their applications.[1–3] Especially, in the field of biosensors polypyrrole derivatives have acquired more importance owing to their biocompatibility, low oxidation potential, high film-forming ability, etc.[4–11] Incorporation of ferrocene to polypyrrole matrices (as mediator) has been particularly examined in order to enhance response of the amperometric biosensors.[12–14] Up to date, several attempts have been made to produce polypyrrole derivatives having covalently attached ferrocene moiety.[15–18] However, synthesis of such polymers through electrochemical polymerization was found to be tricky where in most cases it was only accomplished through electrochemical copolymerization in the presence of similar heterocyclic units not having ferrocene unit.[19]

Since 2001, there has been a growing interest in click chemistry and it has made a significant impact on material and life sciences.[20] Basic features of click reactions could be summarized as simple – selective chemical reaction with high yields, tolerance to variety of solvents, lack significant byproducts. Copper-catalyzed Huisgen 1,3-dipolar cycloaddition of azides and alkynes could be considered as the flagship of click chemistry which has been widely and successfully applied in modification of surfaces,[21–23] synthesis of compounds with complex architecture.[24–26]

Taking advantage of this high yield reaction, we planned to synthesize a series of pyrrole derivatives having ferrocene moiety and investigated their electrochemical polymerization. For this purpose three novel, ferrocene-functionalized N-alkyl substituted pyrrole derivatives, namely 4-ferrocenyl-1-[3-(pyrrol-1-yl)propyl]-1*H*-1,2,3-triazole (Py3Fc), 4-ferrocenyl-1-[4-(pyrrol-1-yl)butyl]-1*H*-1,2,3-triazole (Py4Fc), and 4-ferrocenyl-1-[6-(pyrrol-1-yl)hexyl]-1*H*-1,2,3-triazole (Py6Fc), were synthesized via 'click chemistry' and characterized by ^{1}H NMR, ^{13}C NMR, FTIR, and high-resolution mass spectra (HRMS) techniques. All the monomers were evaluated for their redox behavior and electrochemical syntheses of ferrocene-tethered polypyrroles were investigated. Moreover, we explored the versatility of the 'click' chemistry and effect of spacer group to introduce ferrocene through post-polymerization functionalization.

CONTACT Pinar Camurlu pcamurlu@akdeniz.edu.tr
Supplemental data for this article can be accessed http://dx.doi.org/10.1080/15685551.2015.1136526.

2. Experimental

2.1. General

Except acetonitrile (ACN), dichloromethane (DCM) and propylene carbonate (PC), all the chemicals were purchased from Aldrich or Merck Chemical as reagent grade. Unless otherwise noted, all materials were used as received. Column chromatography was carried out with SiO_2 60 (particle size 0.040–0.063 mm, 230–400 mesh; Merck) and distilled technical solvents. ACN and DCM were distilled over calcium hydride and kept on 4 Å molecular sieves. Tetrabutylammonium hexafluorophosphate ($TBAPF_6$) and lithium perchlorate ($LiClO_4$) were electroanalytical grade. Ethynylferrocene [27] was synthesized according to literature.

2.2. Equipment

An Ivium stat potentiostat/galvanostat was used to supply potential during electrochemical synthesis and cyclic voltammetry (CV). A Basi MF-2062 Non-aqueous Reference Electrode Kit was used as the Ag/Ag^+ reference electrode in ACN with 0.01 M $AgNO_3$ and 0.1 M $TBAPF_6$. Spectroelectrochemistry studies of the polymer films were performed in a UV-cuvette with three-electrodes placed in the sample compartment of a Thermo Evolution Array UV–vis spectrophotometer. For these studies Pt and Ag wires were used as the counter and reference electrodes, respectively. NMR spectra were recorded with a Bruker Avance Spectrometer at 300 MHz for ^1H NMR, Bruker Spectrospin Avance DPX-400 spectrometer at 400 MHz for ^1H NMR, Varian Inova 500 spectrometer at 500 MHz for ^1H NMR. Chemical shifts (δ) were given relative to tetramethylsilane as the internal standard. HRMS was performed on Finnigan MAT95 mass spectrometer 50–1000 Da. The FTIR spectra were recorded on a Brucker Tensor 27 spectrometer.

2.3. General procedure for synthesis of N-substituted pyrroles (Py-N-Br)

N-substituted pyrroles were synthesized through typical alkaline-mediated coupling reaction between pyrrole and dibromoalkanes. As a first step, pyrrole (20 mmol) and KOH (25 mmol) were mixed at 0 °C for 3 h. Later, a solution of 60 mmol dibromoalkane (1,3-dibromopropane, 1,4-dibromobutane, or 1,6-dibromohexane) in DMF (40 mL) was added dropwise to this mixture. The resulting solution was stirred for 12 h at 0 °C and then it was extracted with Et_2O/H_2O, dried $MgSO_4$, and purified by SiO_2 chromatography (20:1 hexane/ethyl acetate). For Py3Br (Yield: 51%): ^1H NMR (300 MHz, $CDCl_3$) (δ/ppm): 6.71 (d, J = 1.93 Hz, 2H), 6.20 (t, J = 2.0 Hz, 2H), 4.11 (t, J = 6.38 Hz, 2H), 3.34 (t, J = 6.19 Hz, 2H), 2.29 (m, 2H) (Figure S1). ^{13}C NMR (75 MHz, $CDCl_3$) (δ/ppm): 120.68, 108.46, 47.08, 34.23, 30.32 (Figure S2). For Py4Br (Yield: 54%): ^1H NMR (400 MHz, $CDCl_3$) (δ/ppm): 6.57 (t, J = 2.08 Hz, 2H), 6.07 (t, J = 2.09 Hz, 2H), 3.85 (t, J = 6.75 Hz, 2H), 3.30 (t, J = 6.44 Hz, 2H), 1.86 (m, 2H), 1.76 (m, 2H) (Figure S5). ^{13}C NMR (101 MHz, $CDCl_3$) (δ/ppm): 119.39, 107.17, 47.67, 31.95, 29.02, 28.78 (Figure S6). For Py6Br (Yield: 43%): ^1H NMR (300 MHz, $CDCl_3$) (δ/ppm): 6.71 (t, J = 2.68 Hz, 2H), 6.21 (t, J = 2.76 Hz, 2H), 3.94 (t, J = 7.06 Hz, 2H), 3.45 (t, J = 6.74 Hz, 2H), 1.87 (m, 4H), 1.52 (m, 4H) (Figure S9). ^{13}C NMR (75 MHz, $CDCl_3$) (δ/ppm): 120.54, 108.04, 49.51, 33.93, 32.75, 31.55, 27.86, 26.03 (Figure S10).

2.4. General procedure for synthesis of azido pyrroles

About 1 mmol Py-N-Br and 10 mmol of NaN_3 were mixed at 50 °C for 6 h in 10 mL of DMF. After cooling to the room temperature, the reaction mixture was partitioned between water and DCM, and the aqueous phase was washed with DCM. The combined organic extracts were washed with concentrated $NaHCO_3$, brine, and dried with $MgSO_4$.[28] The crude product was purified by chromatography (10:1 hexane/ethyl acetate). For $Py3N_3$ (Yield: 82%): ^1H NMR (300 MHz, $CDCl_3$) (δ/ppm): 6.68 (t, J = 2.54 Hz, 2H), 6.19 (t, J = 2.6 Hz, 2H), 4.02 (t, J = 6.65 Hz, 2H), 3.28 (t, J = 6.42 Hz, 2H), 2.03 (m, 2H) (Figure S3). ^{13}C NMR (75 MHz, $CDCl_3$) (δ/ppm): 120.60, 108.44, 48.29, 46.21, 30.73 (Figure S4). For $Py4N_3$ (Yield: 84%): ^1H NMR (400 MHz, $CDCl_3$) (δ/ppm): 6.69 (t, J = 2.06 Hz, 2H), 6.19 (t, J = 2.08 Hz, 2H), 3.95 (t, J = 6.9 Hz, 2H), 3.30 (t, J = 6.73 Hz, 2H), 1.88 (m, 2H), 1.60 ppm (m, 2H) (Figure S7). ^{13}C NMR (101 MHz, $CDCl_3$) (δ/ppm): 120.46, 108.20, 51.04, 49.07, 28.76, 26.24 (Figure S8). For $Py6N_3$ (Yield: 73%): ^1H NMR (300 MHz, $CDCl_3$) (δ/ppm): 6.70 (t, J = 2.04 Hz, 2H), 6.20 (t, J = 2.08 Hz, 2H), 3.93 (t, J = 7.06 Hz, 2H), 3.30 (t, J = 6.82 Hz, 2H), 1.84 (m, 2H), 1.65 (m, 2H), 1.43 (m, 2H) (Figure S11). ^{13}C NMR (75 MHz, $CDCl_3$) (δ/ppm): 120.50, 108.00, 51.37, 49.47, 31.54, 28.82, 26.37 (Figure S12).

2.5. General procedure for click chemistry

$Py3N_3$, $Py4N_3$ or $Py6N_3$ (0.5 mmol) and ethynylferrocene (0.5 mmol) were dissolved in H_2O/THF (1:1, 10 mL), aqueous $CuSO_4{\cdot}5H_2O$ (0.42 mL, 1.0 M), and sodium ascorbate (0.86 mL, 1.0 M) were added and the reaction mixture was stirred at room temperature for 3 h. The resulting mixture was diluted with DCM (100 mL) and the organic phase was separated. The aqueous phase was extracted with DCM (2 × 50 mL). The combined organic phases were washed with brine and dried over $MgSO_4$ and filtered. After removal of the solvent under reduced pressure, the residue was subjected to purification by chromatography on silica gel

(ethyl acetate). For Py3Fc (Yield: 60%): ^{1}H NMR (300 MHz, $CDCl_3$) (δ/ppm): 7.37 (s, 1H), 6.70 (t, J = 2.07 Hz, 2H), 6.21 (t, J = 2.07 Hz, 2H), 4.73 (t, J = 1.88 Hz, 2H), 4.25–4.34 (m, 5H), 4.09 (s, 4H), 3.99 (t, J = 6.59 Hz, 3H), 2.44 (J = 6.59 Hz, 3H). For Py4Fc (Yield: 57%): ^{1}H NMR (300 MHz, $CDCl_3$) (δ/ppm): 7.37 (s, 1H), 6.65 (t, J = 1.99 Hz, 2H), 6.17 (m, 2H), 4.72 (m, 2H), 4.32 (m, 4H), 4.08 (s, 5H), 3.94 (t, J = 6.42 Hz, 2H), 1.91 (m, 2H), 1.81 (m, 2H) (Figure S13). ^{13}C NMR (75 MHz, $CDCl_3$) (δ/ppm): 146.85, 120.48, 118.66, 108.38, 75.43, 69.58, 68.68, 66.62, 49.58, 48.81, 28.37, 27.49 (Figure S14). FTIR (KBr, cm^{-1}): 3117, 3078, 2957, 2924, 2865, 1586, 1497, 1467, 1459, 1359, 1279, 1214, 1105, 1094, 1048, 1028, 999, 879, 831, 817, 736, 720, 615. MS. $C_{20}H_{20}FeN_4$ (m/z) calculated: 375.127, found: 375.125. For Py6Fc (Yield: 48%): ^{1}H NMR (500 MHz, $CDCl_3$) (δ/ppm): 7.41 (s, 1H), 6.63 (t, J = 2.07 Hz, 2H), 6.13 (t, J = 2.07 Hz, 2H), 4.71 (t, J = 2.09 Hz, 2H), 4.32 (t, J = 7 Hz, 2H), 4.29 (t, J = 2.09 Hz, 2H), 4.07 (s, 5H), 3.86 (t, J = 7 Hz, 2H), 1.91 (p, J = 7 Hz, 2H), 1.76 (p, J = 7 Hz, 2H), 1.33–1.34 (m, 4H) (Figure S15). ^{13}C NMR (125 MHz, $CDCl_3$) (δ/ppm): 146.63, 120.27, 118.52, 107.74, 75.38, 69.36, 68.44, 66.42, 49.81, 49.17, 31.12, 29.93, 25.93, 25.88 (Figure S16). FTIR (KBr, cm^{-1}): 3083, 2934, 2857, 1591, 1499, 1469, 1437, 1279, 1213, 1105, 1090, 1053, 825, 730. MS. $C_{22}H_{24}FeN_4$ (m/z) calculated: 402.150, found: 402.149.

2.6. Synthesis of polymers

The electrochemical polymerizations were carried out in a single compartment cell containing 0.01 M monomer and 0.1 M $TBAPF_6$ in 10:1 DCM/ACN or in pure DCM. All polymers were synthesized during potentiodynamic cycling between –0.5 and 1.2 V. Platinum wire or ITO-coated glass can be used as working electrodes. The counter and reference electrodes were a platinum wire and Ag/Ag^+, respectively. After the polymerization, the polymer was rinsed with fresh ACN and characterized by electrochemical and spectral methods.

2.7. Post-polymerization functionalization of P(Py-N_3) derivatives ferrocene

In order to anchor ferrocene to azide-containing polypyrroles (P(Py-N_3)) a classical click reaction was performed, where P(Py-N_3) coated ITO electrodes were soaked in 5 mL ethanol/water (1:1) solution containing 0.1 M ethynylferrocene, 1.0 M $CuSO_4$ and 1.0 M sodium ascorbate at room temperature for 24 h. Subsequently, the electrodes were thoroughly washed with methanol and distilled water, dried under vacuum to remove adsorbed ethynylferrocene. Later on these polymers were subjected to CV and FTIR analyses.

3. Results and discussion

3.1. Synthesis of pyrrole derivatives

In order to explore the effect of spacer group on electrochemical polymerization of ferrocene clicked pyrroles and modification of polypyrrole-coated electrodes, three different *N*-substituted pyrrole derivatives were synthesized via alkaline-mediated coupling reaction between pyrrole and dibromoalkanes in the presence of KOH. Later, the resultant bromine containing pyrroles were subjected to excessive NaN_3 to yield azido-pyrroles (Py3N_3, Py4N_3, Py6N_3). As the final step, copper(I)-catalyzed azide-alkyne Huisgen 1,3-dipolar cycloaddition reaction between ethynylferrocene and azido-pyrroles were carried out under common 'click' conditions to afford ferrocene-tethered pyrroles (Py3Fc, Py4Fc, Py6Fc) (Scheme 1). Chemical structures of all monomers were thoroughly proved by ^{1}H NMR, ^{13}C NMR, FTIR spectra, and HRMS analysis.

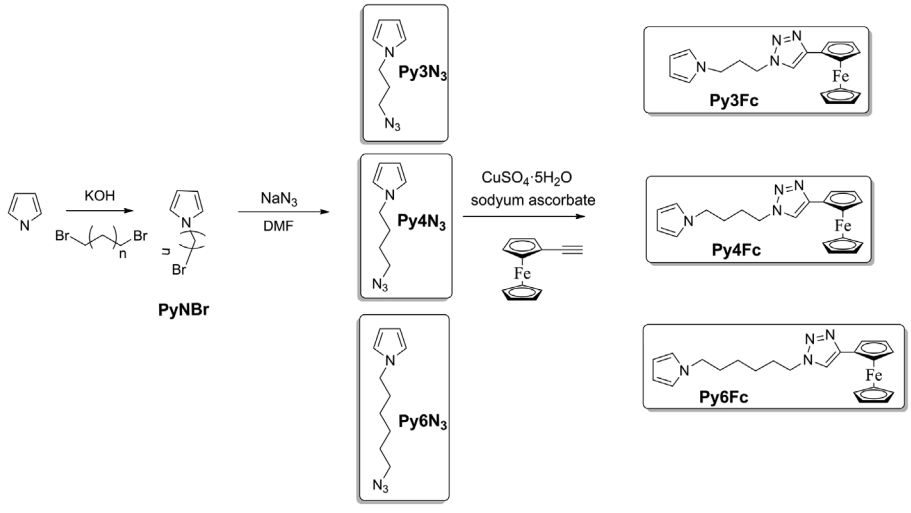

Scheme 1. Synthetic route to monomers.

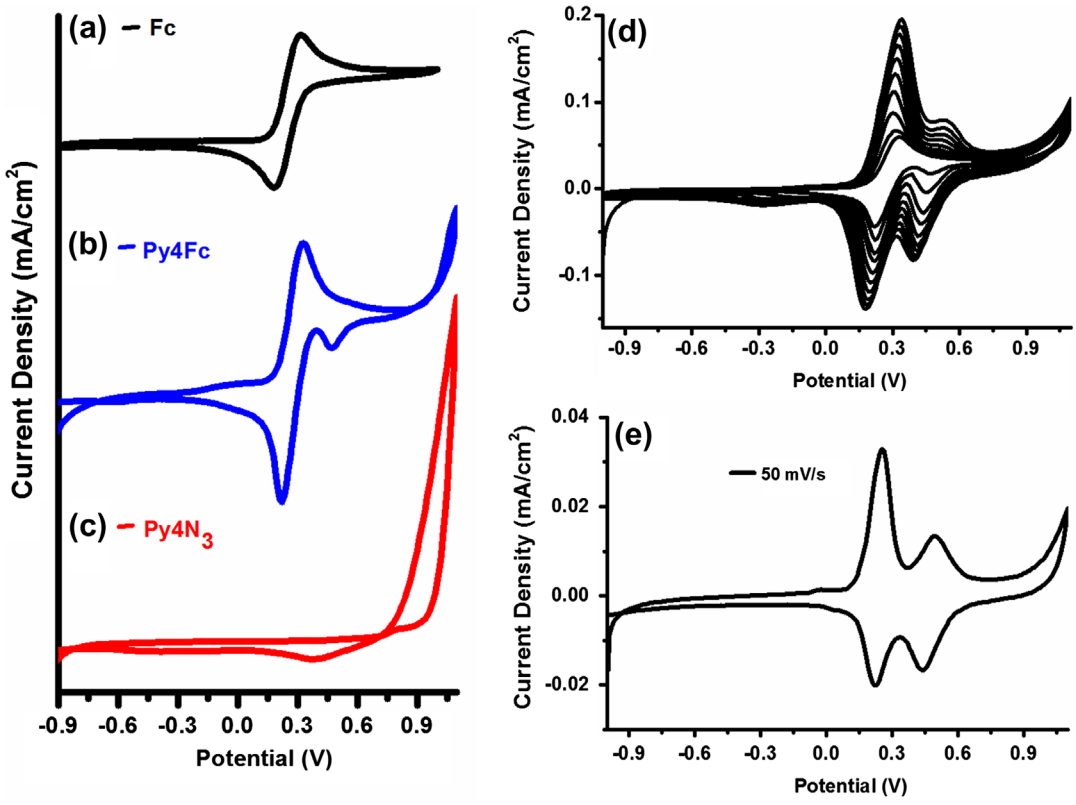

Figure 1. Cyclic voltammogram of (a) pure ferrocene, (b) **Py4Fc**, (c) **Py4N$_3$** (d) **Py4Fc** (multiple cycle) at 100 mV/s^{-1} (e) **P(Py4Fc)** at a scan rate of 50 mV/s in DCM/ACN/TBAPF$_6$ on Pt working electrode, Ag/Ag$^+$ (0.01 M $AgNO_3$, 0.1 M TBAPF$_6$/ACN) reference electrode.

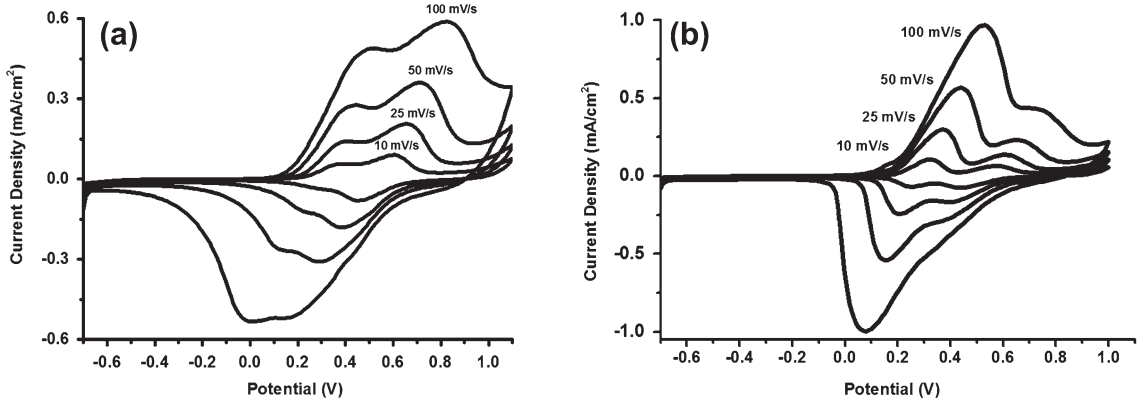

Figure 2. Cyclic voltammogram of **P(Py4Fc)** on ITO at various scan rates (a) in DCM/ACN/TBAPF$_6$, (b) in ACN/TBAPF$_6$.

3.2. Electrochemical properties of ferrocene-anchored pyrroles

The presence of low potential reversible redox signals (around $E_{1/2} = 0.2$ V) in all monomers is consistent with the electrochemical properties of ferrocene, which is known to exhibit reversible redox process (around $E_{1/2} = 0.25$ V, Figure 1(a)). Both Py3Fc and Py4Fc revealed a single reversible redox couple in TBAPF$_6$/ACN system without any significant current increase at the higher potential range and without formation of polymer on the electrode surface. On the other hand, it was possible to graft the conductive films of Py4Fc on Pt electrode in ACN/DCM (1:10) solvent mixture. As seen in Figure 1(b) Py4Fc revealed a reversible redox couple ($E_{½} = 0.27$ V) which is similar to pure ferrocene (Figure 1(a)) in the same media. Amplification of the polarization potential beyond 1.0 V resulted in a steady increase in the current density indicating formation of radical cation of pyrrole unit.[29,30] Such behavior is in accordance with literature [31–33] and Py4N$_3$ as seen in Figure 1(c). Starting from the second scan (Figure 1(d)), a new quasi

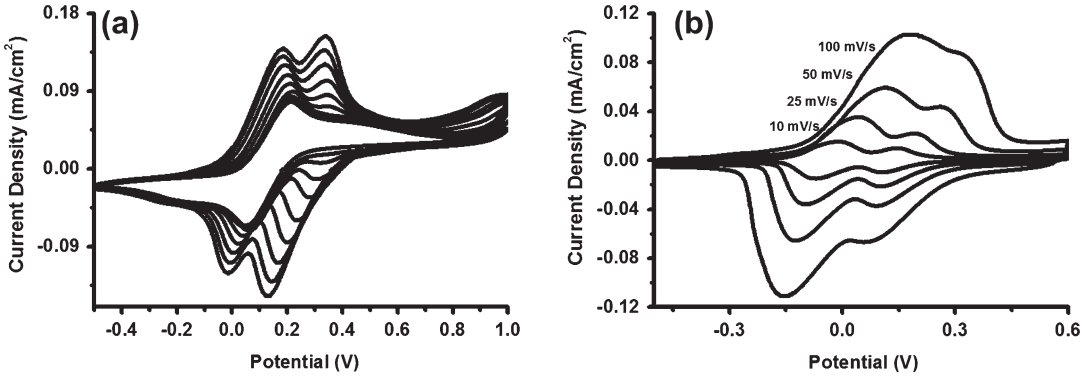

Figure 3. Cyclic voltammogram of (a) **Py6Fc** at 100 mV/s^{-1}, (b) **P(Py6Fc)** at various scan rates on ITO in DCM/TBAPF$_6$.

reversible redox couple was observed in the higher potential range ($E_{P,ox}$ = 0.51 V) which is due to doping–dedoping process of polypyrrole backbone. Moreover, increase in the electrode area was evident by the steady increase in the current density with increasing number of cycles for both redox processes. The presence of polypyrrole-based capasitative response assured the formation of a polymer without significant defects. Formation of electroactive, ferrocene containing P(Py4Fc) film was further supported by voltammogram (Figure 1(e)) which were conducted in monomer-free TBAPF$_6$/ACN/DCM media. Moreover, a direct correlation between the current intensities and scan rate was observed for both ferrocene (R^2_{anodic} = 0.987, $R^2_{cathodic}$ = 0.984) and polymer backbone (R^2_{anodic} = 0.999, $R^2_{cathodic}$ = 0.999) related processes in TBAPF$_6$/ACN/DCM electrolyte system (Figure S20). Similar type of results was achieved for the studies conducted in the same polymerization media with ITO electrode, which is suitable for post-polymerization studies. However, it was interesting to see the effect of solvent on the relative current intensities of ferrocene and polymer backbone-related redox processes for the polymers that were synthesized on ITO under identical conditions. As we could see the ratio of the former to the later process is higher than one for the polymers characterized in DCM/ACN system (Figure 2(a)), which is lower than one in ACN (Figure 2(b)). Such effect presumably originates from the difference in the solubility parameters of the solvents, leading to a variation in degree of swelling and availability of the active sites. In order to explore the effect of solvent on the redox behavior of Py4Fc, further studies were conducted in TBAPF$_6$/DCM system. As in the case of ACN/DCM mixture system, in DCM Py4Fc revealed a well-defined reversible redox process at around 0.3 V and an irreversible oxidation at beyond 0.9 V, where the former process is attributed to its ferrocene moiety and the later signified the formation of radical cation of the monomer (Figure S18). However, contrary to ACN/DCM solvent system, upon continuous cycling the color of the solution in the vicinity of the working electrode changed and a homogeneous, adherent thin film was not achieved. This again could be related to the higher solvation power of DCM which prevents precipitation of polymer on electrode and leads to leakage of the oligomers in to the polymerization media.

Contrary to Py4Fc, despite varying the polarization potential, the electrode type (Pt, ITO), the supporting electrolyte (LiClO$_4$, TBAPF$_6$) and the solvent (DCM, ACN, PC) it was not possible to electrochemically polymerize Py3Fc. Following the first scan, Py3Fc revealed ill-defined redox behavior presumably due to interaction of ferrocenium ion (Fc^+) with radical cation of pyrrole, whereby inhibiting the oxidative coupling of radical cations (Figure S17).[16,34]

Figure 3(a) represents the cyclic voltammogram of Py6Fc in TBAPF$_6$/DCM. As we could see Py6Fc revealed two well-defined reversible redox process with peak potentials of $E_{ox,1}$: 0.21 V and $E_{ox,2}$: 0.35 V. Following several potentiodynamic switches between −0.5 and 1.0 V, an electroactive, well-adhered polymer film [35] readily deposited on ITO electrode, which showed linear increase in current densities with increase in scan rate (Figure 3(b), Figure S21). Contrary to other ferrocene-containing pyrroles in the literature [19,36,37] both Py4Fc and Py6Fc were readily polymerizable without requiring the presence of a comonomer for polymerization to take place. Moreover, since the ferrocene unit is separated by the relatively long spacer groups, for both polymers it was possible to see the individual redox processes stemming from the polypyrrole and ferrocene units, which is not valid for most of the former studies.[18,38,39] However, despite their well-defined quasi-reversible redox activity on ITO electrodes, none of the ferrocene-containing polypyrroles (P(Py4Fc), P(Py6Fc)) displayed significant spectral (color) variations during repetitive redox switches between neutral and oxidized states. Optical band gap of (P(Py4Fc)) was estimated as 2.75 eV, which was calculated through the lower energy absorption edge of the spectrum.

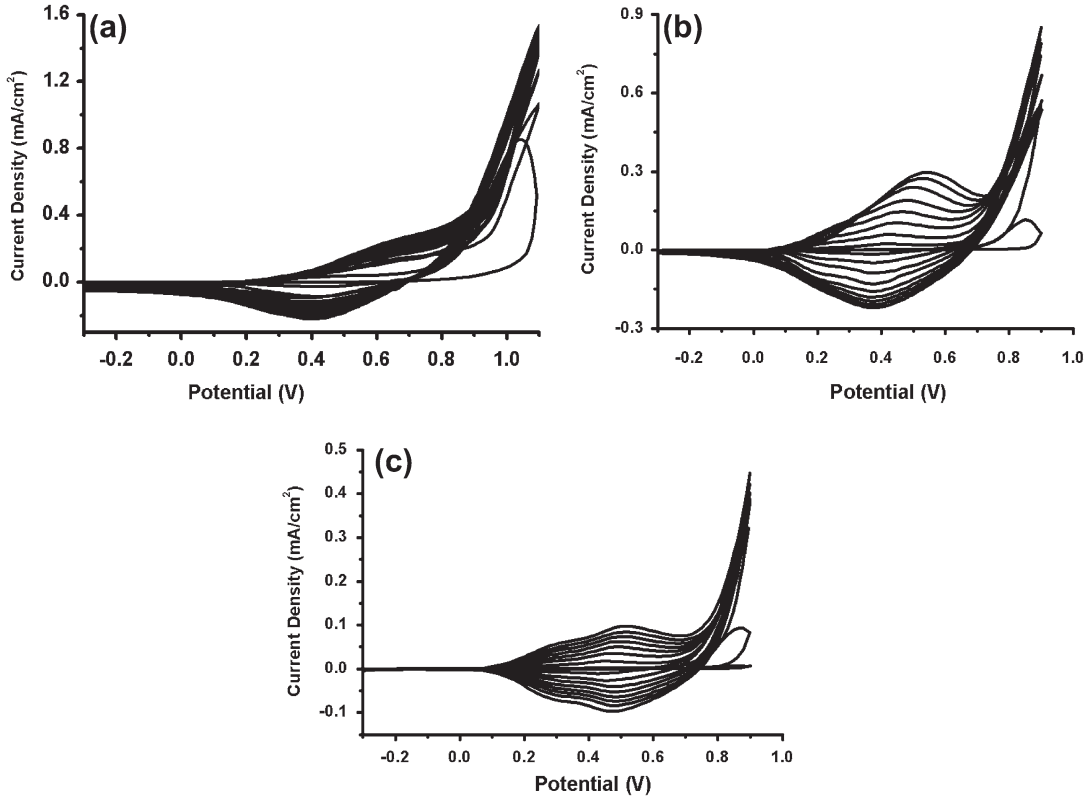

Figure 4. Cyclic voltammogram of (a) **Py3N$_3$**, (b) **Py4N$_3$** and (c) **Py6N$_3$** at 100 mV/s^{-1} in DCM/TBAPF$_6$, where Pt wire, Ag/Ag$^+$ and ITO were used as the counter electrode, reference electrode and working electrode, respectively.

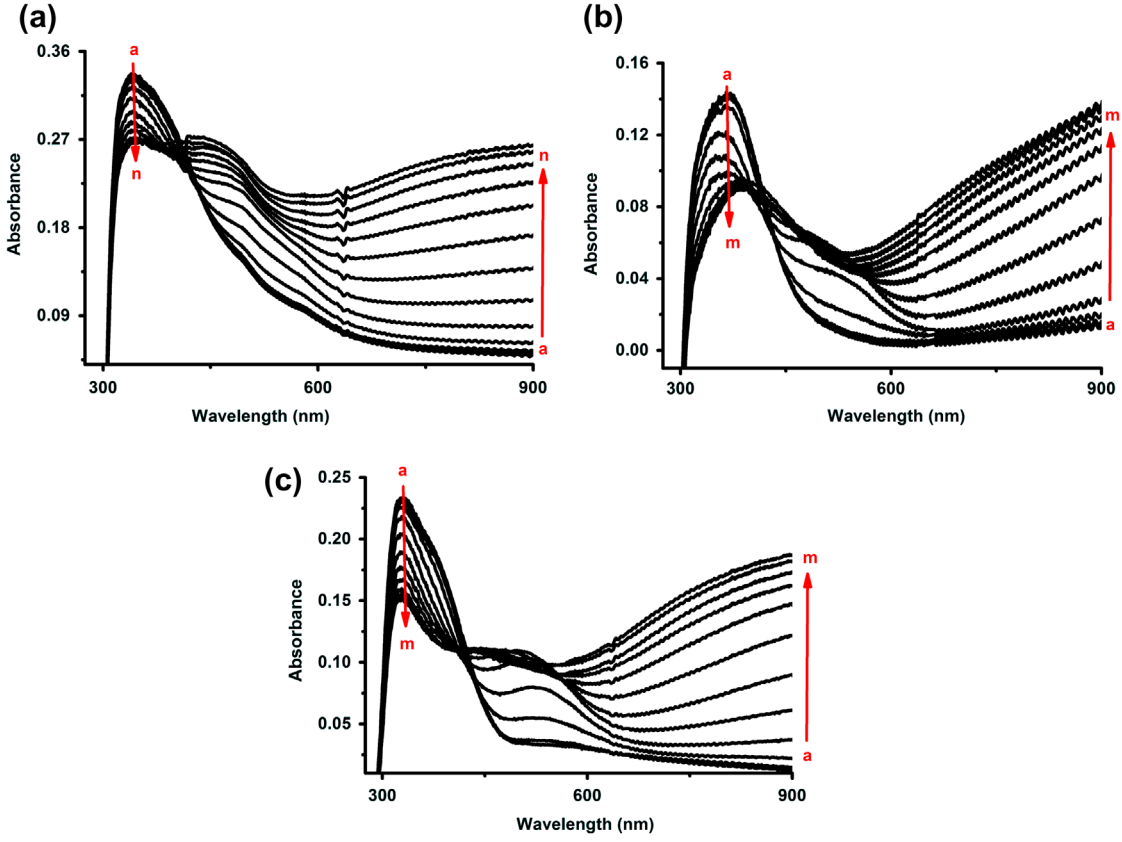

Figure 5. Spectroelectrochemistry of (a) **P(Py3N$_3$)**, (b) **P(Py4N$_3$)** and (c) **P(Py6N$_3$)** in DCM/TBAPF$_6$ at applied potentials between −0.5 and 1.1 V (a: −0.5 V, b: −0.2 V, c: 0.0 V, d: 0.1 V, e: 0.2 V, f: 0.3 V, g: 0.4 V, h: 0.5 V, i: 0.6 V, j: 0.7 V, k: 0.8 V, l: 0.9 V, m: 1.0 V, n: 1.1 V).

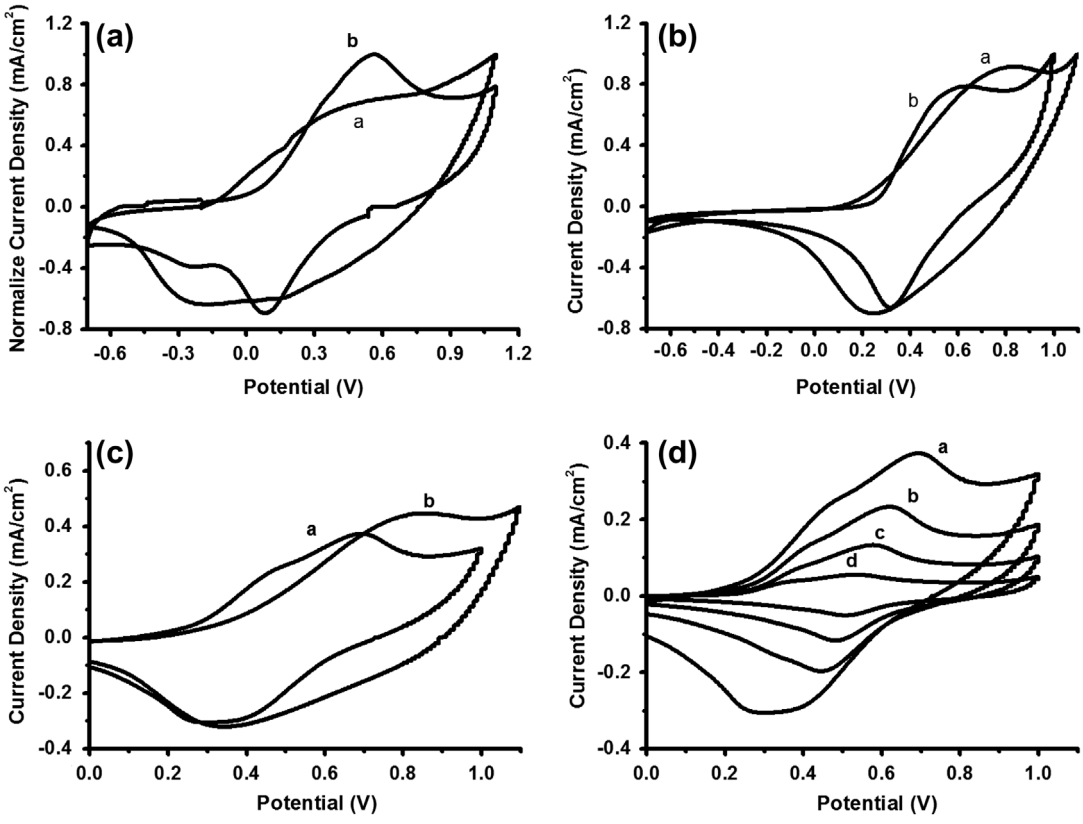

Figure 6. Cyclic voltammogram of (a) a: **P(Py3N$_3$)**, b: **P(Py3-post-Fc)** in DCM/TBAPF$_6$, (b) a: **P(Py4N$_3$)**, b: **P(Py4-post-Fc)** in DCM/TBAPF$_6$, (c) a: **P(Py6-post-Fc)**, b: **P(Py6N$_3$)** in ACN/LiClO$_4$, (d) **P(Py6-post-Fc)** at various scan rates in ACN/LiClO$_4$ (a: 100 mV/s, b:50 mV/s, c: 25 mV/s, d: 10 mV/s).

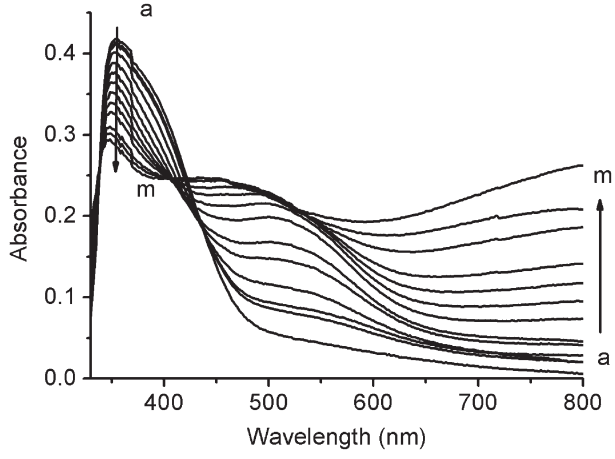

Figure 7. Spectroelectrochemistry of **P(Py6-post-Fc)** in ACN/LiClO$_4$ at applied potentials between 0.0 and 1.0 V (a: 0.0 V, b: 0.2 V, c: 0.3 V, d: 0.4 V, e: 0.45 V, f: 0.5 V, g: 0.55 V, h: 0.6 V, i: 0.65 V, j: 0.7 V, k: 0.8 V, l: 0.9 V, m: 1.0 V).

3.3. Post-polymerization functionalization of azide-containing pyrroles

Being one of the major advantages of the click chemistry, we performed post-polymerization functionalization of the polypyrrole derivatives through azide groups. For this purpose, we have investigated the redox properties of all Py-N-N$_3$ (Py3N$_3$, Py4N$_3$, Py6N$_3$) derivatives. As seen Figure 4 all the monomers revealed an irreversible oxidation beyond 0.85 V, which is typical for *N*-substituted pyrroles. Formation of azide-containing polypyrroles (P(Py-N-N$_3$)) were followed by the gradual increase in the current upon repetitive cycling and by the growth of a new redox process emerging at around 0.5 V due to the doping–dedoping of polypyrrole backbone. Once the polymer films were formed they were subjected to CV studies in a fresh, monomer-free electrolyte solution at various scan rates (Figure S19). All the polymers revealed the typical surface confined redox behavior where a linear dependence between the current and scan rate is observed (Figure S22). Moreover, existence of the strong peak at around 2090 cm^{-1} in FTIR spectra of all P(Py-N-N$_3$) derivatives indicated the unperturbed presence of azide groups during polymerization.

The UV–vis absorption spectra of P(Py-N-N$_3$) films (Figure 5) showed two absorption bands at 330–365 and 470–525 nm at applied potentials between –0.5 and 1.1 V. The former broad absorption band is typical for π–π^* transitions, which dominates the optical behavior of the polymer at neutral state, and they are in good agreement with previous studies.[40] The optical gap band of P(Py3N$_3$),

P(Py4N_3), P(Py6N_3) are calculated as 2.37, 2.61, 2.67 eV, respectively. As the oxidation proceeds, the later transitions in the spectrum became dominant indicating the generation of charge carrier bands inside the band gap. As typical of *N*-substituted polypyrrole derivatives, these polymers also could be oxidized up to a certain level by means of simple electrochemical oxidation. Contrary to P(Py4N_3), P(Py6N_3), these polymer films displayed reversible color transition between brownish yellow and blue upon switching.

Later on, these polymers were subjected to a simple click reaction with ethynylferrocene in 1.0 M $CuSO_4$, 1.0 M sodium ascorbate ethanol/water (1:1) media for 24 h. [41,42] After washing thoroughly with methanol (to eliminate the effect of adsorbed alkyne) the polypyrrole films (P(Py-N-post-Fc)) were characterized by electrochemical methods and FTIR. Figures 6(a)–(c) represents the CV of P(Py3-post-Fc), P(Py4-post-Fc) and P(Py6-post-Fc) and their azido polypyrrole (P(Py3N_3), P(Py4N_3), P(Py6N_3)) analogs, which were treated under click conditions without the presence of ethynylferrocene, respectively. As we could see, the former two (P(Py3-post-Fc), P(Py4-post-Fc)) displayed very similar redox behavior to their azido derivatives. P(Py6-post-Fc), on the other hand, revealed two quasi-reversible redox couples at around $E_{p,1/2}$ = 0.37 and $E_{p,1/2}$ = 0.53 V as in the case of P(Py6Fc). The former redox couple at lower potential range could be attributed to ferrocene units and later couple could be related to doping of polypyrrole main chain (Figure 6(d)). The higher reversibility and better peak separation in the CV of P(Py6Fc) could stem from the presence higher amount of ferrocene (one for each pyrrole unit) in the bulk of the polymer, whereas in post-polymerization functionalization mainly anchoring on the surface of the film is expected. Thus, current intensity and reversibility of the redox couples (especially those related to ferrocene units) are less defined in case of P(Py6-post-Fc) than P(Py6Fc).

Moreover, when compared with FTIR spectrum of P(Py6N_3), P(Py6-post-Fc) revealed a significant reduction in the strong IR signal at 2090 cm^{-1} (azide stretching) and presence of new peaks at 480 cm^{-1} due to covalent bonding of ferrocene unit (Fe/C bond vibration). Thus, CV and FTIR studies afforded solid evidence of post-polymerization functionalization only for P(Py6N_3) electrode, where effective tethering of ferrocene seems to depend on length of spacer group. The optoelectronic properties of P(Py6-post-Fc) was investigated in 0.1 M $LiClO_4$/ACN solution (Figure 7). While amplifying the potential from 0.0 to 1.0 V, intensity of the absorption peak at 355 nm (due to π–π^* transition) decreased and simultaneously a new the absorption peak around 510 nm intensified due to formation of charge carrier bands. These results are in accordance with P(Py6N_3), which underlines the fact that contrary to P(Py6Fc), P(Py6-post-Fc) can be reversibly doped and de-doped with a well-defined electrochromic response. Hence, through utilization of post-polymerization functionalization it was possible to achieve an electrochromic, ferrocene-containing polypyrrole derivative.

4. Conclusion

This study demonstrates a detailed investigation on synthesis of ferrocene-anchored polypyrroles through alternative approach. Our methodology utilizes the versatility of the click chemistry and considers the effect of spacer group between pyrrole and ferrocene units both during monomer synthesis and post-polymerization functionalization stages. Our studies indicated the importance of the spacer group, which played a key role in electrochemical polymerization process by providing the opportunity for the essential pyrrole-based radical cation coupling step to take place. Contrary to literature studies, where polymerization is mainly achieved by electrochemical copolymerization, with this approach it was possible to synthesize homopolymers of pyrrole derivatives having covalently bonded ferrocene units. Furthermore, three different electrochemically synthesized azide-containing polypyrroles were subjected to click reaction in the presence of ethynylferrocene, where effective clicking (anchoring) was only achieved in case of longest spacer group. Future studies are on the way for utilization of these ferrocene-containing polymers in biosensor applications.

Disclosure statement

No potential conflict of interest was reported by the authors.

Funding

This work was supported by TUBITAK [Project No: 110T640].

References

[1] Yuan X, Ding X-L, Wang C-Y, et al. Use of polypyrrole in catalysts for low temperature fuel cells. Energy Environ. Sci. 2013;6:1105–1124.
[2] Geetha S, Rao CRK, Vijayan M, et al. Biosensing and drug delivery by polypyrrole. Anal. Chim. Acta. 2006;568:119–125.
[4] Camurlu P. Polypyrrole derivatives for electrochromic applications. RSC Adv. 2014;4:55832–55845.
[4] Ramanavičius A, Ramanavičienė A, Malinauskas A. Electrochemical sensors based on conducting polymer – polypyrrole. Electrochim. Acta. 2006;51:6025–6037.
[5] Wang J, Musameh M. Carbon-nanotubes doped polypyrrole glucose biosensor. Anal. Chim. Acta. 2005;539:209–213.

[6] Razola SS, Ruiz BL, Diez NM, et al. Hydrogen peroxide sensitive amperometric biosensor based on horseradish peroxidase entrapped in a polypyrrole electrode. Biosens. Bioelectron. 2002;17:921–928.
[7] Habermüller K, Ramanavicius A, Laurinavicius V, et al. An oxygen-insensitive reagentless glucose biosensor based on osmium-complex modified polypyrrole. Electroanalysis. 2000;12:1383–1389.
[8] Brahim S, Narinesingh D, Guiseppi-Elie A. Polypyrrole-hydrogel composites for the construction of clinically important biosensors. Biosens. Bioelectron. 2002;17:53–59.
[9] Komaba S, Seyama M, Momma T, et al. Potentiometric biosensor for urea based on electropolymerized electroinactive polypyrrole. Electrochim. Acta. 1997;42:383–388.
[10] Sahmetlioglu E, Yürük H, Toppare L, et al. Immobilization of invertase and glucose oxidase in conducting copolymers of thiophene functionalized poly(vinyl alcohol) with pyrrole. React. Funct. Polym. 2006;66:365–371.
[11] Cosnier S, Senillou A, Gratzel M, et al. A glucose biosensor based on enzyme entrapment within polypyrrole films electrodeposited on mesoporous titanium dioxide. J. Electroanal. Chem. 1999;469:176–181.
[12] Geetha S, Rao CRK, Vijayan M, et al. Biosensing and drug delivery by polypyrrole. Anal. Chim. Acta. 2006;568:119–125.
[13] Schuhmann W. Electron-transfer pathways in amperometric biosensors. Ferrocene-modified enzymes entrapped in conducting-polymer layers. Biosens. Bioelectron. 1995;10:181–193.
[14] Kesik M, Akbulut H, Söylemez S, et al. Synthesis and characterization of conducting polymers containing polypeptide and ferrocene side chains as ethanol biosensors. Polym. Chem. 2014;5:6295–6306.
[15] Vidal JC, Garcia E, Castillo JR. Development of a platinized and ferrocene-mediated cholesterol amperometric biosensor based on electropolymerization of polypyrrole in a flow system. Anal. Sci. 2002;18:537–542.
[16] Foulds NC, Lowe CR. Immobilization of glucose oxidase in ferrocene-modified pyrrole polymers. Anal. Chem. 1988;60:2473–2478.
[17] Zotti G, Zecchin S, Schiavon G. Conductivity in redox modified conducting polymers. 2. Enhanced redox conductivity in ferrocene-substituted polypyrroles and polythiophenes. Chem. Mater. 1995;7:2309–2315.
[18] Saint-Aman E, Ungureanu M, Visan T, et al. Investigation of electrochemical reversibility and redox-active polypyrrole film formation of amide ferrocene-pyrrole derivatives. Electrochim. Acta. 1997;42:1829–1837.
[19] Moutet JC, Saint-Aman E, Ungureanu M, et al. Electropolymerization of ferrocene bis-amide derivatives: a possible route to an electrochemical sensory device. J. Electroanal. Chem. 1996;410:79–85.
[20] Chen J, Too CO, Wallace GG, et al. Redox-active conducting polymers incorporating ferrocenes. Preparation, characterization and bio-sensing properties of ferrocenylpropyl and -butyl polypyrroles. Electrochim. Acta. 2002;47:4227–4238.
[21] Kolb HC, Finn MG, Sharpless KB. Click chemistry: Diverse chemical function from a few good reactions. Angew. Chem. Int. Ed.. 2001;40:2004–2021.
[22] Arnusch CJ, Branderhorst H, de Kruijff B, et al. Enhanced membrane pore formation by multimeric/oligomeric antimicrobial peptides. Biochemistry. 2007;46:13437–13442.
[23] Ortega-Munoz M, Morales-Sanfrutos J, Perez-Balderas F, et al. Click multivalent neoglycoconjugates as synthetic activators in cell adhesion and stimulation of monocyte/machrophage cell lines. Org. Biomol. Chem. 2007;5:2291–2301.
[24] Vestberg R, Malkoch M, Kade M, et al. Role of architecture and molecular weight in the formation of tailor-made ultrathin multilayers using dendritic macromolecules and click chemistry. J. Polym. Sci. Part A: Polym. Chem. 2007;45:2835–2846.
[25] Doran S, Murtezi E, Barlas FB, et al. One-pot photo-induced sequential CuAAC and thiol–ene click strategy for bioactive macromolecular synthesis. Macromolecules. 2014;47:3608–3613.
[26] Ak M, Gacal B, Kiskan B, et al. Enhancing electrochromic properties of polypyrrole by silsesquioxane nanocages. Polymer. 2008;49:2202–2210.
[27] Ossipov DA, Hilborn J. Poly(vinyl alcohol)-based hydrogels formed by "Click Chemistry". Macromolecules. 2006;39:1709–1718.
[28] Polin J, Schottenberger H. Conversion of methyl ketones into terminal acetylenes: ethynylferrocene. Org. Synth. 1998;9:411–415.
[29] Camurlu P, Karagoren N. Clickable, versatile poly(2,5-dithienylpyrrole)derivatives. React. Funct. Polym. 2014;73:847–853.
[30] Cernat A, Griveau S, Martin P, et al. Electrografted nanostructured platforms for click chemistry. Electrochem. Commun. 2012;23:141–144.
[31] Li Y, Zhang W, Chang J, et al. "Click" on conducting polymer coated electrodes: a versatile platform for the modification of electrode surfaces. Macromol. Chem. Phys. 2008;209:322–329.
[32] Calvo-Muñoz ML, Bile BEA, Billon M, et al. Electrochemical study by a redox probe of the chemical post-functionalization of N-substituted polypyrrole films: application of a new approach to immobilization of biotinylated molecules. J. Electroanal. Chem. 2005;578:301–313.
[33] Ion AC, Moutet JC, Pailleret A, et al. Electrochemical recognition of metal cations by poly(crown ether ferrocene) films investigated by cyclic voltammetry and electrochemical impedance spectroscopy. J. Electroanal. Chem. 1999;464:24–30.
[34] Camurlu P, Eren E, Gültekin C. A solution-processible, n-dopable polypyrrole derivative. J. Polym. Sci., Part A: Polym. Chem. 2012;50:4847–4853.
[35] Zotti G, Schiavon G, Zecchin S, et al. Self-assembly and electropolymerization of pyrrole- and bithiophene-*n*-hexyl-ferrocene molecules on ITO electrodes. Synth. Met. 1997;84:239–240.
[36] Kumar A, Welsh DM, Morvant MC, et al. Conducting poly(3,4-alkylenedioxythiophene) derivatives as fast electrochromics with high-contrast ratios. Chem. Mater. 1998;10:896–902.
[37] Soon GH, Deasy M, Worsfold O, et al. Synthesis, co-polymerization, and electrochemical evaluation of novel ferrocene-pyrrole derivatives. Anal. Lett. 2011;44:1976–1995.

[38] Chen J, Too CO, Wallace GG, et al. Redox-active conducting polymers incorporating ferrocenes 2. Preparation and characterization of polypyrroles containing propyl- and buthyl-tethered [1.1] ferrocenophane. Electrochim. Acta. 2004;49:691–702.
[39] Baüerle P, Hiller M, Scheib S, et al. Post-polymerization functionalization of conducting polymers: novel poly(alkylthiophene)s substituted with easily. Replaceable activated ester groups. Adv. Mater. 1996;8:214–218.
[40] Reynes O, Royal G, Chaînet E, et al. Poly(ferrocenylalkylammonium): a molecular electrode material for dihydrogenphosphate sensing. Electroanalysis. 2003;15:65–69.
[41] Fermín DJ, Teruel H, Scharifker BR. Changes in the population of neutral species and charge carriers during electrochemical oxidation of polypyrrole. J. Electroanal. Chem. 1996;401:207–214.
[42] Bicil Z, Camurlu P, Yucel B, et al. Multichromic, ferrocene clicked poly(2,5-dithienylpyrrole)s. J. Polym. Res. 2013;20:228.
[43] Xu J, Tian Y, Peng R, et al. Ferrocene clicked poly(3,4-ethylenedioxythiophene) conducting polymer: characterization, electrochemical and electrochromic properties. Electrochem. Commun. 2009;11:1972–1975.